

## Role of the Atmosphere in Climate Variability of the Tropical Atlantic

ALFREDO RUIZ-BARRADAS, JAMES A. CARTON, AND SUMANT NIGAM

*Department of Meteorology, University of Maryland, College Park, Maryland*

(Manuscript received 7 May 2001, in final form 13 October 2002)

### ABSTRACT

This paper explores climate variability of the lower troposphere and boundary layer in the tropical Atlantic sector through a series of modeling simulations with a diagnostic primitive equation model. The focus is on the role that realistic diabatic heating and its vertical placement as well as surface temperature have in inducing/reinforcing the local monthly wind circulation, the role that thermal and momentum transients play in the Tropics, the potential for feedbacks, and the way through which other basins influence the tropical Atlantic region. NCEP–NCAR reanalysis data for the period 1958–93 are used to provide forcing and model verification.

In the first part of the paper local effects are considered. It is found that the most important terms controlling anomalous surface winds over the ocean are boundary layer temperature gradients and diabatic heating anomalies at low levels (below 780 mb). Anomalous diabatic heating at mid- and upper levels (430–690 mb) contributes to the near-surface circulation poleward of  $15^\circ$  over the warm hemisphere. Anomalous diabatic heating over the African continent influences zonal winds well into the ocean. It is found that the anomalies of surface latent heat flux induced by the interhemispheric distribution of anomalies provide positive feedback on both sides of the equator, in the deep Tropics and west of  $20^\circ\text{W}$ . It provides negative feedback off the northwest coast of Africa.

In the second part the relative importance of remote forcing is considered. It is found that anomalous heating associated with interhemispheric gradients of surface temperature in the tropical Atlantic influence winds in the northern extratropics in a wavelike pattern during boreal spring. Anomalous heating associated with equatorial anomalies of surface temperature influence winds in the southern extratropics in a wavelike pattern during boreal summer. In contrast, the influence of heating in the midlatitudes is confined to the northern subtropics. Anomalous ENSO-related diabatic heating influences near-surface winds in the tropical Atlantic, which resembles the local response to interhemispheric gradients of surface temperature. This remote influence induces changes in the intensity of the Atlantic Walker and Hadley circulations as a consequence of the direct effect of heating in the eastern tropical Pacific.

### 1. Introduction

In this paper we explore the role of the atmosphere in climate variability in the tropical Atlantic sector. Some previous studies have suggested a variety of potential mechanisms by which variability is produced by local interactions within this sector (e.g., Hastenrath 1978; Moura and Shukla 1981; Wagner and da Silva 1994). Other studies have implicated remote forcing as the ultimate source of variability (e.g., Nobre and Shukla 1996; Enfield and Mayer 1997; Tanimoto and Xie 1999; Saravanan and Chang 2000; Sutton et al. 2000a; Chang et al. 2001). In either case the atmosphere's response in the tropical Atlantic is complicated by the presence of zones of intense convection over the Amazon and central Africa and small-scale rapid variations in the structure of the troposphere throughout the basin. Here we explore the impact of these unusual features through a

series of simulations with a diagnostic primitive equation model.

The near-surface winds of the tropical Atlantic are dominated by the southeast and northeast trade winds systems, which converge at the intertropical convergence zone (ITCZ). Large spatial gradients in sea surface temperature (SST) resulting from the shallow thermocline and complex geometry of the Atlantic lead to large pressure gradients in the planetary boundary layer, which play an important role in controlling seasonal surface winds (Philander 1990). In addition, transients and diabatic heating contribute to the general behavior of the tropical winds. Momentum and thermal transients result from the daily meandering of the subtropical jets and their seasonal shifts in latitude that can go as far equatorward as  $\sim 15^\circ$  latitude in both hemispheres. These transients seem to have a minor effect in the deep tropical Atlantic at surface levels but have some influence in the subtropical regions at upper levels,  $\sim 200$  mb (Peixoto and Oort 1995). Diabatic heating anomalies are associated with movements of the ITCZ. The level of maximum variance of (residually diagnosed) diabatic

---

*Corresponding author address:* Alfredo Ruiz-Barradas, 3420 Computer and Space Sciences Bldg., Department of Meteorology, University of Maryland, College Park, MD 20742-2425.  
E-mail: alfredo@atmos.umd.edu

heating is higher and deeper over continents ( $\sim 500$  mb) than over the ocean ( $\sim 800$ – $900$  mb). In addition to meridional shifting with season, diabatic heating also shifts in the zonal direction following the shift of warm SST ( $27^{\circ}\text{C}$ ) from west in boreal spring to east in boreal summer. In the west convection is concentrated between  $5^{\circ}\text{S}$ – $5^{\circ}\text{N}$  and extends high into the atmosphere ( $\sim 550$ – $200$  mb). On each side of the basin convection extends over the adjacent continent (across cool coastal waters in the east). The western side has the lowest change with season while the eastern side experiences the highest change.

The convective zones are dominated by tall clouds resulting in a deepening of the planetary boundary layer to 2 km. In the ITCZ itself rain rates exceeding  $10\text{ mm day}^{-1}$  are not uncommon, while shallow boundary layers (500 m) and shallow clouds are prevalent in the eastern ocean north and south of the ITCZ. These latter clouds result in significant low-level radiative cooling. Additional cooling may result from evaporating rain. Thus, one of the key differences in the heating profiles of the Atlantic in comparison with the eastern Pacific is the presence of both low-level and deep heating in close proximity (Ruiz-Barradas et al. 2000, hereafter R-BCN).

The interannual and decadal variability of the tropical Atlantic has attracted considerable attention; much of it focusing on variability associated with local SST variations. Many studies beginning with Hastenrath (1978) have suggested the existence of a coupled mode of variability associated with interhemispheric differences in SST and a meridional displacement of the ITCZ toward the warmer hemisphere (the interhemispheric mode of R-BCN). Examination of rainfall distributions by Moura and Shukla (1981) and weather center analyses by Hastenrath and Greischar (1993) suggest the importance of diabatic heating due to convective clouds, while the recent modeling studies of Chang et al. (2000) and Chiang et al. (2001) and principal component analyses of R-BCN suggest the importance of low-level heating anomalies within the boundary layer. Diabatic heating has the potential of influencing near-surface winds depending on its vertical distribution (Wu et al. 2000). In a recent paper Chiang et al. (2001) conclude that SST gradients, in a distribution of anomalies with an interhemispheric SST gradient, control meridional winds close to the equator while elevated heating ( $\sim 700$  mb) controls the surface zonal wind response everywhere plus the subtropical surface meridional wind. Here we revisit the issue of the impact of low-level heating anomalies on the near-surface circulation. Modeling studies by Carton et al. (1996) show changes in surface winds may influence SST anomalies in a way that reinforces the initial anomaly, an idea whose importance in regulating SST is supported by Chang et al. (2000) but in conflict with Sutton et al. (2000a).

In addition to variability associated with interhemispheric gradients of SST, the tropical Atlantic is subject

to equatorial temperature anomalies (the Atlantic Niño mode of R-BCN). SST variability in the eastern basin is strongly linked to the seasonal cycle, being most pronounced in boreal summer (Zebiak 1993). Examination of historical rainfall by Carton et al. (1996) and diabatic heating by R-BCN shows that the relaxation of the trade winds to the west of the positive SST anomalies is associated with a southward shift and amplification of convective heating. Here also, however, Wagner and da Silva (1994) argue for the importance of SST's influence on boundary layer pressure gradients.

Other studies have explored remote forcing of the winds of the tropical Atlantic (e.g., Enfield and Mayer 1997; Sutton et al. 2000a; Saravanan and Chang 2000). Enfield and Mayer (1997) note a significant correlation between SST in the tropical Atlantic and ENSO and suggest that a fraction of the interhemispheric variability in the tropical Atlantic is forced by way of an atmospheric bridge. A number of other studies including Curtis and Hastenrath (1995), Nobre and Shukla (1996), Giannini et al. (2000), Saravanan and Chang (2000), Sutton et al. (2000a), and Mestas-Núñez and Enfield (2001) have also suggested such a link along a zone between  $10^{\circ}$ – $20^{\circ}\text{N}$ . In addition, Sutton et al. (2000a), Chiang and Kushnir (2000), and Saravanan and Chang (2000) suggest that the influence from the Pacific is also transmitted through perturbation of the Atlantic Walker circulation. Mestas-Núñez and Enfield (2001), and Rodó (2001) highlight the importance of a weak Atlantic Hadley cell as a response to anomalous warming in the eastern tropical Pacific. Sutton et al. (2000a) further suggest that those competing mechanisms may contribute to the weakening of the Atlantic Hadley cell during boreal winter. Here, we explore these issues through the use of a linear model that allow us to separate the influences of the tropical Pacific and Atlantic more easily, and explore the roles of the purely tropical and mid-latitudes responses.

The effect of the North Atlantic on the tropical Atlantic has been suggested by Tanimoto and Xie (1999). However, results by Rajagopalan et al. (1998), Robertson et al. (2000), and Watanabe and Kimoto (1999) suggest that the influence is from the Tropics to the midlatitudes during boreal winter. The North Atlantic Oscillation (NAO), defined here as the surface air pressure difference between the Azores and Iceland, reflects basinwide changes in the strength and orientation of the North Atlantic jet stream and storm track and consequently also the position and strength of the mid-Atlantic westerlies. Results by Sutton et al. (2000a) indicate that the NAO can perturb the poleward side of the northeast trade winds, especially during boreal winter. In another study Sutton et al. (2000b) shows that SST anomalies in the northern tropical Atlantic can affect the NAO region during the same winter season. Watanabe and Kimoto (1999) suggest that under the influence of those winter SST anomalies the forcing in the midlatitudes is organized by the associated heating

in the tropical Atlantic with transients contributing the most in the generation of the midlatitudes response. Chang et al. (2001) suggests that although local air–sea feedbacks in the deep Tropics generate the pattern of interhemispheric SST gradient and cross-equatorial surface winds, the instability is weak requiring external forcing such as the NAO-related “noise” to excite the coupled variability. In the present study we also explore the possible atmospheric connection between the Tropics and extratropics but centered on boreal spring and summer when the tropical Atlantic modes present their maximum amplitude.

## 2. The model and its forcing

The diagnostic primitive equation model used here solves the steady sigma coordinate primitive equations for momentum obtained from linearization about a zonally symmetric basic state. The resulting linear equations model the eddy component of the circulation (Held et al. 1989; Nigam 1994, 1997). The equations are solved numerically on a sphere using a semispectral representation of the horizontal structure with  $2.5^\circ$  meridional resolution and 30 zonal wavenumbers (approximately  $6^\circ$  zonal resolution). The vertical structure is discretized using 18 full sigma levels of which 14 are in the troposphere, including 5 below 850 mb. Rayleigh momentum-dissipation and Newtonian temperature-damping terms in the equations are replaced by a linearized version of vertical diffusion terms (Nigam 1997), which include momentum and thermal vertical diffusion coefficients. The inclusion of the vertical diffusion terms requires the specification of additional linear boundary conditions for the momentum and thermodynamic equations. In addition to boundary layer dissipation the momentum and thermodynamic equations include a horizontal  $\nabla^2$  diffusive damping, and a sponge layer near the model top to dissipate vertical reflections from above.

The friction coefficients were chosen to match zonal and meridional wind anomalies in the bands  $7.5^\circ\text{S}$ – $0^\circ$  and  $0^\circ$ – $7.5^\circ\text{N}$  as well as the pattern of surface pressure anomalies for the Atlantic Niño and interhemispheric modes of R-BCN over the ocean. The drag coefficient was chosen to be  $C_D = 1 \times 10^{-3}$ . Preliminary simulations show that reduction of this coefficient increases the zonal component of the wind but stretches the pressure pattern unrealistically in the zonal direction. The vertical diffusion coefficient was chosen to be  $\nu_v = 30 \{1 + \tanh[10\pi(\sigma - 0.850)]\} \text{ m}^2 \text{ s}^{-1}$ . Additional simulations show that this term does not have an important effect on the surface fields. Horizontal diffusion was chosen to be  $\nu = 3 \times 10^5 \text{ m}^2 \text{ s}^{-1}$ . Simulations with different values of horizontal diffusion show that low values tend to spread surface pressure anomalies beyond the tropical Atlantic zonally as well as meridionally. Maximum values of winds are considerably reduced,

with the reduction more noticeable at upper levels than at the surface.

The basic state of zonally averaged winds, density, and temperature is obtained from the time-average of the National Centers for Environmental Prediction–National Center for Atmospheric Research (NCEP–NCAR) reanalysis dataset (Kalnay et al. 1996) for the period 1958–93. Orography has been obtained from the European Centre for Medium-Range Weather Forecasts (ECMWF) dataset with  $2.5^\circ \times 2.5^\circ$  resolution. This forcing appears in the lower boundary condition used in the vertical integration of the hydrostatic equation providing a mechanical forcing to the circulation. Orography is not included as a high source of sensible heating (i.e., radiative forcing). A set of experiments showed little orographic effects in our region of interest, but a strong dependence on the basic state. The model anomalies are forced three ways—through diabatic heating and transient eddy heat fluxes, which drive the heat equation; through eddy momentum fluxes, which drive the momentum equations; and through anomalous surface temperature and topography, which drive the boundary layer. Transients have been obtained from the daily NCEP reanalysis dataset for the period 1958–93. Diabatic heating has been residually diagnosed through the thermodynamic equation (e.g., Nigam 1997).

In this study we also explore thermodynamic feedbacks so we calculate latent heat anomalies from simulated winds. Surface latent heat flux anomalies are calculated from a bulk formula  $LE' = L\rho C_e [V_a(q^* - q)_a - V_c(q^* - q)_c]$  with the saturation specific humidity given by the formula  $q^* = 0.622 \times e_s(T_s)/P$ , where  $e_s(T_s) = 6.112 \exp\{17.67[T_s/(T_s + 243.5)]\}$ . Here,  $L = 2.5 \times 10^6 \text{ J kg}^{-1}$  is the latent heat of evaporation,  $\rho = 1.225 \text{ kg m}^{-3}$  is the density of the air,  $C_e = 1.35 \times 10^{-3}$  is the latent heat transfer coefficient,  $V$  is the wind speed in  $\text{m s}^{-1}$ ,  $q$  is the specific humidity,  $e_s$  is the saturation vapor pressure in mb, at surface temperature  $T_s$ , in  $^\circ\text{C}$ ,  $P$  is the surface pressure in mb, and  $(\ )_a$  and  $(\ )_c$  denote anomalous and climatological monthly values. The saturation specific humidity is calculated in terms of the saturation vapor pressure, which in turn is calculated using an empirical relationship following Bolton (1980), while surface temperature, pressure, and specific humidity are obtained from the NCEP reanalysis regressions and the winds are derived from model simulations.

As mentioned in the introduction the strongest fluctuations in the wind field are associated with the annual meridional and zonal shifts of the ITCZ, as well as changes in convection over the Amazon and the waxing and waning of the West African monsoon. Here we begin testing the response of the model by comparing its seasonal cycle with observations in the extreme seasons of boreal spring and summer (Figs. 1 and 2). In this and in subsequent comparisons we focus on surface variables, particularly winds because of their obvious relevance to coupled ocean–atmosphere interactions, and



## Mean March–April–May

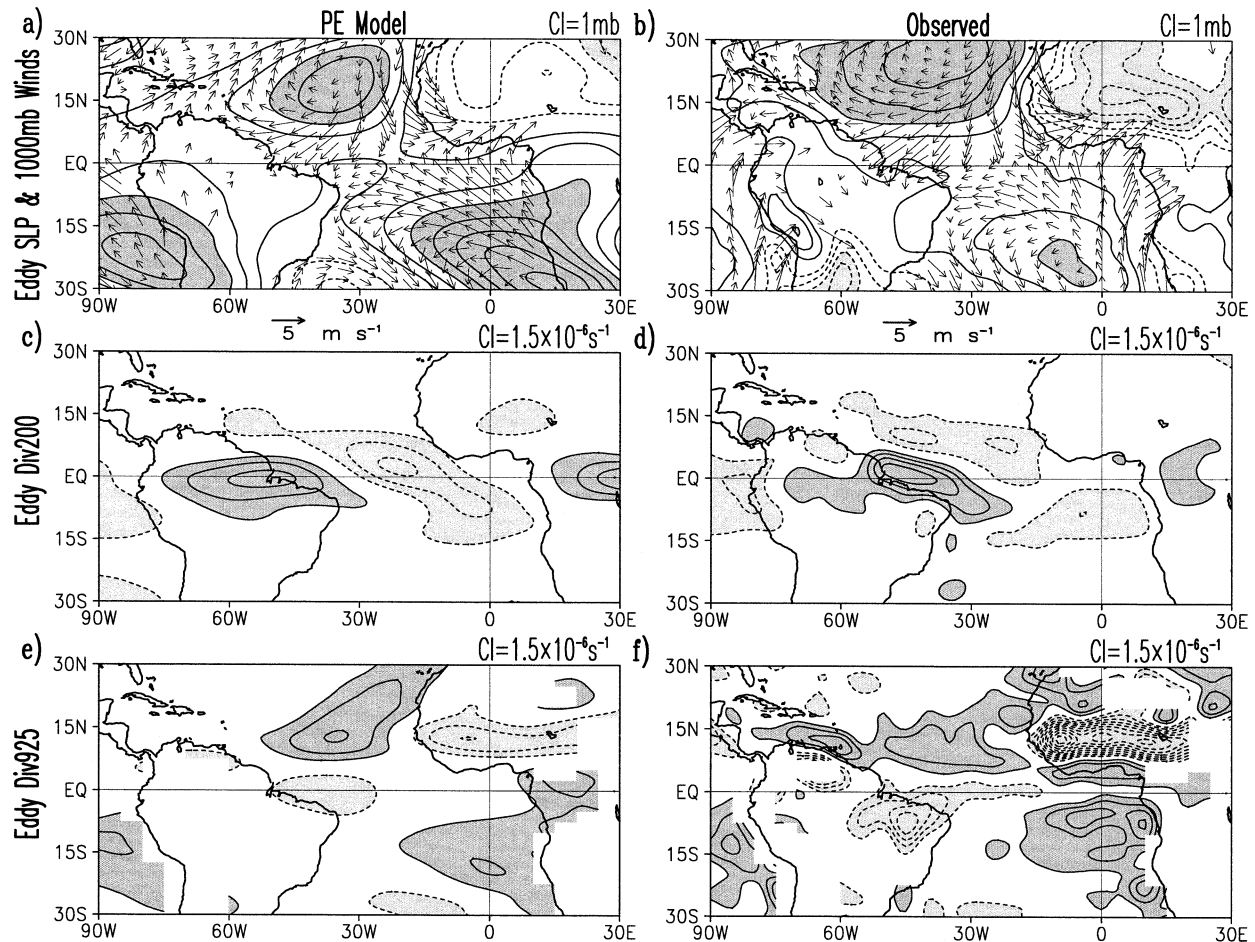


FIG. 1. Mean Mar–May simulation using the linear primitive equation (PE) model and observations from NCEP reanalysis data. (a) Simulated eddy sea level pressure (mb) and winds ( $\text{m s}^{-1}$ ) at 1000 mb. (b) Observed fields corresponding to (a). (c) Simulated eddy divergence ( $10^{-7} \text{ s}^{-1}$ ) at 200 mb. (d) Observed fields corresponding to (c). (e) Eddy divergence ( $10^{-7} \text{ s}^{-1}$ ) at 925 mb. (f) Observed fields corresponding to (e). Climatology is calculated for the period 1958–93. Dark (light) shading denotes positive (negative) eddies larger than  $\pm 3 \text{ mb}$  for pressure and  $\pm 1.5 \times 10^{-6} \text{ s}^{-1}$  for divergence.

200-mb winds because of the potential role that the upper troposphere may play in interaction between basins. We have chosen to compare 1000-mb winds rather than winds stress because of the enhanced sensitivity of the latter to the choice of surface drag formulation.

In summary, the model is quite successful in simulating observed variability and in particular the annual progression of the ITCZ and the strength and direction of the northeast and southeast trade winds systems. The exception to this occurs over South America in boreal spring. During that season continental heating leads to an observed reduction in surface pressure and development of a cyclonic circulation. However, the model surface pressure over this region is high and consequently surface winds are anticyclonic. Inclusion of orography does not improve the simulation. The ITCZ itself is not as intense as observed and as a consequence

the zones of near-surface divergence associated with the Hadley and Walker circulations are also not as intense as observed. At 200 mb the comparison is also quite good, again with the exception of South America in boreal summer. During this season the model shows a distinct pattern of divergence, while the observations show a disorderly pattern of convergences and divergences.

We complete our examination of the model by determining its tropical response to anomalies from the seasonal cycle. In this simulation the model is forced with the observed monthly anomalies of global diabatic heating, transient momentum and heat fluxes, and surface temperature obtained from the reanalysis dataset, as described earlier. We then correlate the simulated and observed surface wind anomalies over the full 36-yr record. The results presented in Fig. 3 show correlations

## Mean June–July–August

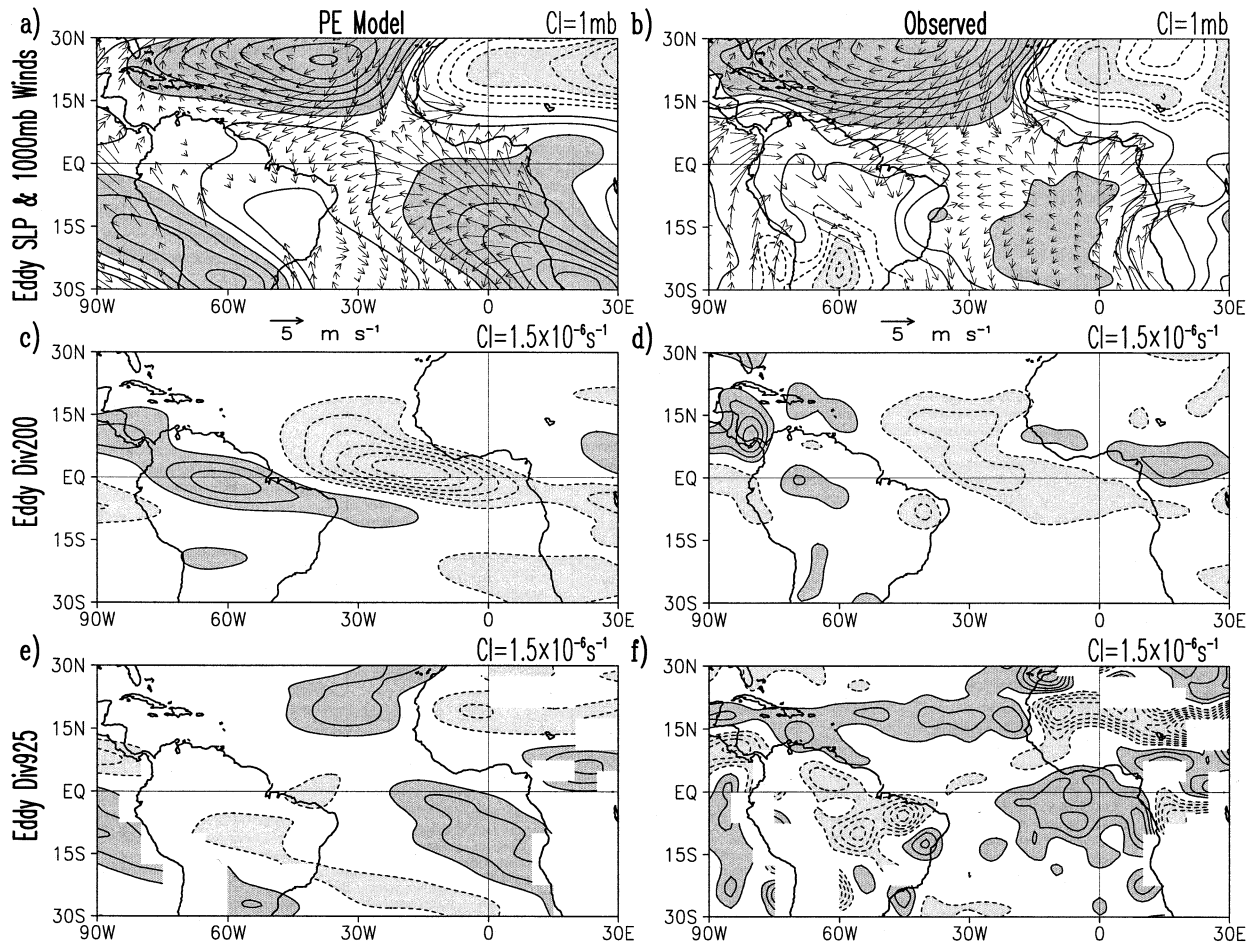


FIG. 2. The same as in Fig. 1 but for mean Jun–Aug.

generally exceeding 0.5 over the tropical ocean with poorer agreement over land and over the cool waters of the southeast. The results are considerably improved over those of simple empirical or dynamical models (Chung et al. 2002). The reduced correlation over land may result from the complexity and time-dependence of hydrologic and meteorological conditions there, which are not well represented by our model. The reduced correlations over the cool oceanic upwelling zones may indicate difficulties in both the model and the reanalysis in resolving surface winds under stratus cloud conditions where the boundary layer is shallow and the trade winds inversion is strong.

As described in the introduction, two modes of interannual/decadal variability have been discussed in the tropical Atlantic. Here we compare the observed structure of these modes with simulated structures as a way of characterizing the response of the model atmosphere to broad tropical heating as well as to heating confined to the deep Tropics over the 36-yr period. The structure of surface temperature, as well as that of diabatic heating

and transients for these modes, has been determined by regressing those fields on the corresponding principal components (time series) of the modes during the season in which they dominate (R-BCN)—boreal spring, (March–May) for the interhemispheric mode and boreal summer (June–August) for the Atlantic Niño mode. Throughout the rest of this paper we use the distribution of heating, boundary layer temperature, and transients for the interhemispheric (i.e., interhemispheric distribution of anomalies) and Atlantic Niño (i.e., equatorial distribution of anomalies) modes to explore the atmospheric response, which are not homogeneous in space.

The interhemispheric distribution of anomalies is characterized by strong anomalies of surface temperature in the northern tropical Atlantic and weak anomalies with the opposite sign in the southern Tropics during boreal spring. These anomalies extend eastward over northern Africa. When the northern tropical Atlantic is warmer than the southern one the ITCZ over the western basin is anomalously displaced to the north. Interestingly, a meridional profile of diabatic heating anomalies



### Wind anomaly correlations (From Global Forcing)

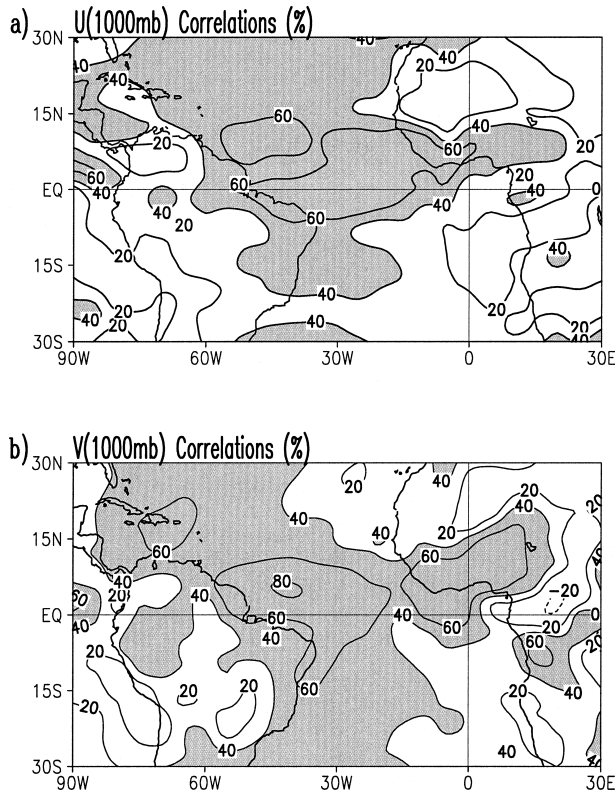


FIG. 3. Correlations between NCEP reanalysis wind anomalies and those simulated with the linear PE model for the (a) zonal and (b) meridional components when the model is forced with global anomalous diabatic heating, transients, and surface temperature. Time series span the period 1958–93. Correlations are multiplied by 100. Contour interval is 20% and shading denotes regions where correlations are 40% or higher.

associated with this mode across the western position of the ITCZ has different positive maxima with height, inside the boundary layer (800–900 mb), and in the middle and upper troposphere (500–300 mb).

The equatorial distribution of anomalies, in contrast, is characterized by strong anomalies of surface temperature along the equator mainly confined to the central and eastern sides of the basin with a southern extension during boreal summer. Associated with these surface temperature anomalies, there is also an equatorial distribution of anomalies in diabatic heating that reflects an anomalous placement ( $\sim 7^\circ$  southward of the climatological position) of the ITCZ over the eastern basin. A zonal profile of diabatic heating anomalies along the equator includes a strong low-level vertical gradient in the boundary layer (not maximum inside of it) as well as a midlevel maximum; the former may also contribute to the local circulation.

### 3. Response to local forcing

We now use the model to explore the factors responsible for driving surface winds at interannual to decadal periods. A major theme will be the determination of the relative importance of boundary layer temperature, diabatic heating, and transient momentum and heat fluxes. Because our interest is on the study of “local” anomalies in the tropical Atlantic, we adopt as control simulations those when forcing (diabatic heating as well as momentum and thermal transients and anomalous surface temperature) is confined into the tropical Atlantic ( $20^\circ\text{S}$ – $30^\circ\text{N}$ ,  $80^\circ\text{W}$ – $30^\circ\text{E}$ ). Thus we have one control simulation for the interhemispheric distribution of anomalies and another for the equatorial one. We treat each control simulation as “truth” and focus attention on the differences between any simulation and the corresponding control simulation. We then present a series of simulations testing the potential impact of a given forcing on the circulation of the tropical Atlantic. In each case we estimate this impact by comparing surface winds from the control simulation with winds from simulations in which each potential mechanism is the only forcing.

The control simulation for the interhemispheric distribution of anomalies and its observed anomalies are displayed in Figs. 4a,b. The observed anomalies of the interhemispheric mode are well represented, however, sea level pressure and wind anomalies are  $\sim 50\%$  too weak. The observed 1000-mb winds have a significant ageostrophic component (crossing isobars) between the equator and  $15^\circ\text{N}$ , which is not as pronounced in the control simulation. Thus, the simulated winds are more strongly westerly in this latitude band than observed. Surface latent heat flux anomalies (Fig. 5a) reach maximum values of  $|-14| \text{ W m}^{-2}$ . Recalling that the interhemispheric mode in its positive phase has positive SST anomalies in the northern Tropics, latent heat flux anomalies in the northwestern basin indicate positive feedback in agreement with Chang et al. (2000) [see also Wang and Enfield (2001) for a different mechanism inducing positive feedbacks] but in contrast to Sutton et al. (2000a). In the east, off northwest Africa the feedback is negative, consistent with Chang et al. (2000). The bulk formula for latent heat flux anomalies depends on anomalies of both surface wind and specific humidity. In a study of six AGCMs Wang and Carton (2002, hereafter WC02) note that the negative feedback in the eastern basin may be a spurious result of errors in specific humidity.

The control simulation winds for the equatorial distribution of anomalies and the corresponding observed anomalies (Figs. 4c,d) agree in magnitude and direction with observations. The success of the simulation suggests that extrabasin effects have little effect on this mode. Surface latent heat flux anomalies (Fig. 5b), over equatorial positive SST anomalies, also reach maximum values of  $|-14| \text{ W m}^{-2}$  with positive feedback to the

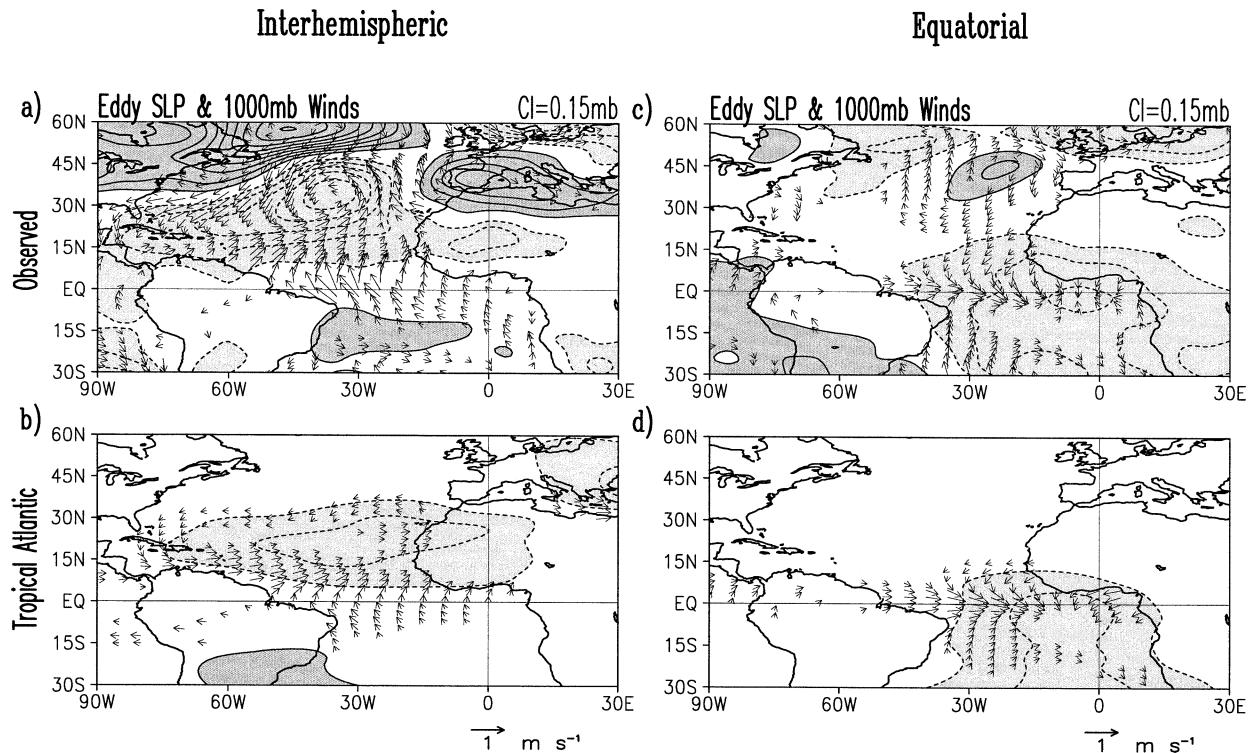


FIG. 4. Observed and simulated eddy fields for the interhemispheric and equatorial distribution of anomalies examining the impact of tropical Atlantic forcing. Eddy anomalies of sea level pressure (mb) and wind ( $\text{m s}^{-1}$ ) at 1000 mb: (a) observed regressed from NCEP reanalysis data and (b) simulated for the interhemispheric distribution of anomalies; (c) observed regressed, and (d) simulated for the equatorial distribution of anomalies. Simulated fields are obtained when complete forcing (i.e., diabatic heating, momentum and thermal transients, and surface temperature) is restricted to the tropical Atlantic ( $20^{\circ}\text{S}$ – $30^{\circ}\text{N}$ ,  $80^{\circ}\text{W}$ – $30^{\circ}\text{E}$ ). Dark (light) shading denotes positive (negative) anomalies larger than  $\pm 0.15$  mb for pressure and  $\pm 2 \times 10^{-7} \text{ s}^{-1}$  for divergence.

west of  $20^{\circ}\text{W}$  and negative feedback to the east. However the short quasi-biennial timescale of the associated mode means that anomalous latent heat flux is not the primary mechanism controlling anomalous equatorial SST.

We now begin our analysis of the impact of different forcing terms. Diabatic heating anomalies of the interhemispheric and equatorial distributions reach their maximum values between 400 and 500 mb, however low-level heating anomalies are also present. Comparing mass-weighted vertically integrated diabatic heating anomalies, we see that for the interhemispheric distribution of anomalies maximum low-level heating anomalies do not lie over the maximum SST anomalies, as is the case for the equatorial distribution of anomalies (Fig. 6). Analysis of surface pressure anomalies and 850–1000-mb thickness indicates that those anomalies are well correlated with anomalous SST (Ruiz-Barradas et al. 2002; see also Hastenrath and Greischar 1993) suggesting the importance of boundary layer processes (Lindzen and Nigam 1987) in controlling anomalous low-level winds. Thus we use the term “surface forcing” to refer to forcing resulting from surface temperature and diabatic heating at low levels (pressure  $\geq 780$  mb), while “elevated forcing” refers to forcing coming

from mid- and upper-level diabatic heating (pressure  $\leq 690$  mb). The final term we explore is forcing due to transients.

We explore the role of these different forcing terms through three simulations. In the first, we omit anomalous diabatic heating and anomalous surface temperature leaving only anomalous transients. In the second, we omit anomalous transients, diabatic heating at lower levels (pressure  $\geq 780$  mb), and surface temperature leaving only anomalous diabatic heating at middle and upper levels (pressure  $\leq 690$  mb), the elevated forcing. Third, we omit anomalous transients and anomalous diabatic heating at upper and middle levels leaving only anomalous diabatic heating at lower levels and anomalous surface temperature, the surface forcing (Figs. 7 and 8).

For the interhemispheric distribution of anomalies we find that there is no anomalous circulation in the deep Tropics in the absence of diabatic heating and surface temperature (Fig. 7a). Anomalous transients produce sea level pressure and wind anomalies with the opposite sign of those produced by diabatic heating in the subtropics. Elevated forcing causes much of the subtropical sea level pressure variability of the interhemispheric distribution and reduces the strength of the northeast trade

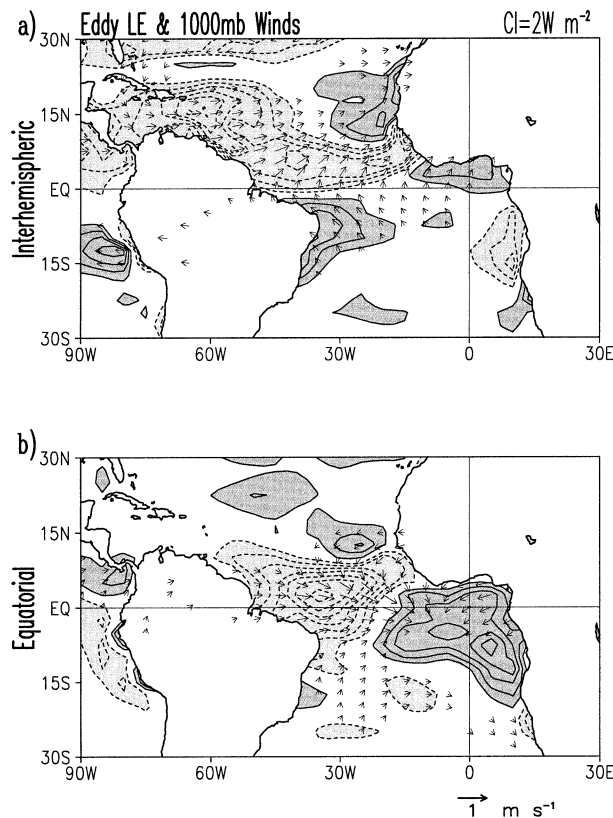


FIG. 5. Latent heat eddy anomalies ( $\text{W m}^{-2}$ ) calculated using winds from the control simulation in the bulk formula for (a) the interhemispheric and (b) the equatorial distribution of anomalies. Arrows represent wind eddy anomalies. Dark (light) shading denotes enhanced (reduced) latent heat flux from the ocean to the atmosphere larger than  $\pm 2 \text{ W m}^{-2}$ .

winds (Fig. 7b). Finally, surface forcing produces cross-equatorial surface winds, while it reduces the strength of the northeast trade winds in the deep Tropics (Fig. 7c). Indeed, the surface forcing alone accounts for 93% of the anomalous meridional, and 88% of the anomalous zonal surface winds averaged along the equatorial bands  $7.5^\circ\text{S}$ – $0^\circ$ – $7.5^\circ\text{N}$ .<sup>1</sup> In contrast, mid- and upper-level diabatic heating accounts for 80% of anomalous meridional and zonal surface winds in the band  $7.5^\circ$ – $15^\circ\text{N}$ , and even more in the rest of the northern subtropical domain.

For the equatorial distribution of anomalies, diabatic heating is also the main forcing of the circulation (Figs. 8a–c) with surface forcing driving surface winds in the deep Tropics. Elevated forcing is important both along the equator in the west and in the subtropical Southern Hemisphere (Fig. 8b) in broadening the extension of the negative sea level pressure anomalies as well as the wind

anomalies. In contrast, surface forcing is responsible for the convergence of surface wind anomalies (Fig. 8c). Surface forcing contributes 56% and 68% to the zonal and meridional surface wind anomalies of the control simulation along the previously defined equatorial band.

We have also explored the effect of anomalous continental diabatic heating using a set of historical simulations (not shown). In the first simulation global anomalous diabatic heating and surface temperature force the circulation, while in the second anomalous diabatic heating is confined to continental areas in the tropical Atlantic region with climatological surface temperature everywhere. The difference between the simulations indicates that continental heating from northern Africa has an important contribution to the surface zonal component of the circulation over much of the northern Tropics through the whole year, but especially during boreal summer and fall. It has an important contribution to the surface meridional component only in the northern region of the Gulf of Guinea. The contribution of continental heating from the Amazon to surface winds is mostly confined to the South American continent. Its contribution is mainly to the meridional component especially during boreal spring and summer. An example of this type of experiment for the simulated interhemispheric distribution of anomalies when forcing is confined in the tropical Atlantic and diabatic heating and surface temperatures are climatological only over the ocean is shown in Fig. 9. It is clear, when comparing with Fig. 4b, that the cyclonic circulation over northwestern Africa favors cross-equatorial wind anomalies eastward of  $\sim 15^\circ\text{W}$  and reduces northward wind anomalies off the subtropical African coasts. The response in the surface wind anomalies results from surface forcing over Africa (cf. Figs. 6a and 6b).

In another set of simulations (not shown) we explore the role transients play by replacing thermal or momentum transients separately with their climatological values and comparing the results to the control simulation (Figs. 4b,d) and with the simulation with only transients (Figs. 7a and 8a). We find that for the interhemispheric distribution of anomalies, anomalous thermal transients produce the positive sea level pressure anomaly over the ocean seen in the transients-only simulation. The contribution of anomalous momentum transients is limited to the region east of  $20^\circ\text{W}$ . For the equatorial distribution of anomalies, momentum transients produce the meridional extension of the minimum sea level pressure and wind between  $15^\circ$ – $30^\circ\text{S}$ —apparent in the control simulation.

#### 4. Remote influences

When global forcing is used the patterns in the tropical Atlantic are more realistic, indicating forcing external to the basin itself is important, particularly for the interhemispheric distribution (cf. Figs. 10a,b with Figs. 4b,d). In this section we explore the tropical mid-

<sup>1</sup> For each wind component of a given experiment a mean value is calculated in the two bands from  $7.5^\circ\text{S}$  to the equator and from the equator to  $7.5^\circ\text{N}$  in the tropical Atlantic. Then a difference is calculated with respect to the mean values of the control simulation and evaluated as a percentage.



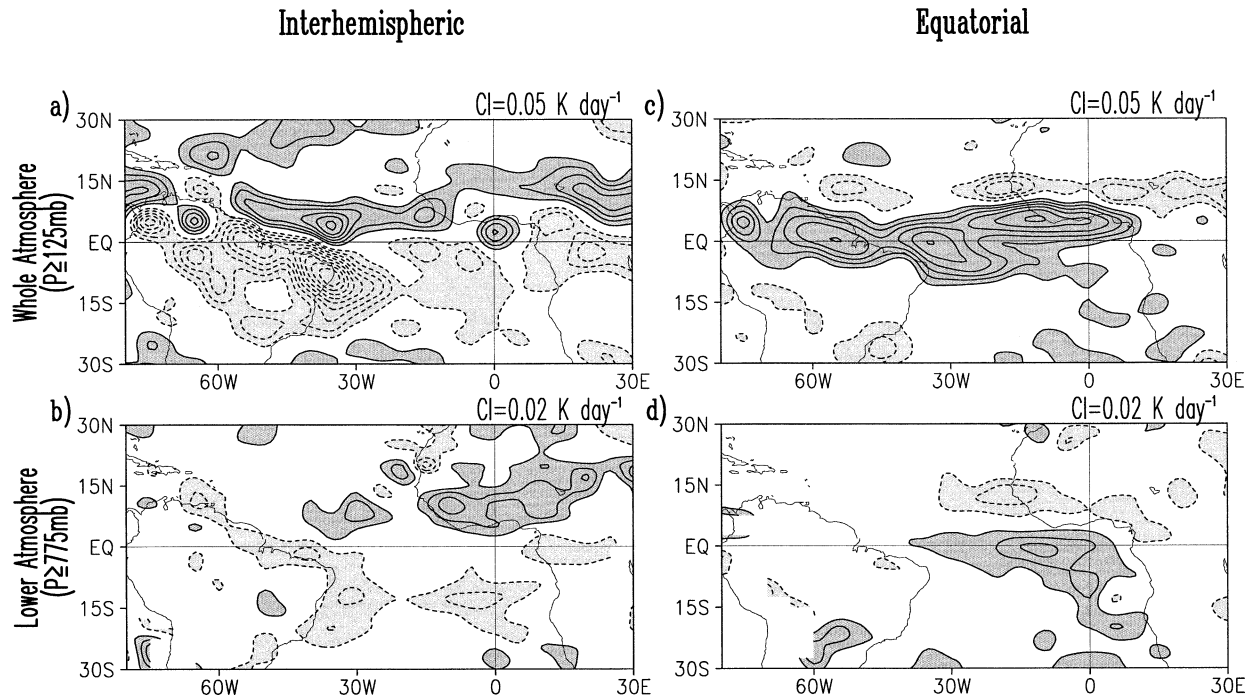


FIG. 6. Mass-weighted vertically integrated diabatic heating anomalies (a) when integration is carried out through the whole atmosphere (pressure  $\geq 100$  mb) and (b) when integration is only through the lower atmosphere (pressure  $\geq 780$  mb) for the interhemispheric distribution of anomalies. (c), (d) Corresponding vertical integrations for the equatorial distribution of anomalies. Dark (light) shading denotes warming (cooling) larger than  $\pm 0.05$  K day $^{-1}$  for integration through the whole atmosphere, and  $\pm 0.02$  K day $^{-1}$  for integration through the lower atmosphere.

latitudes and the tropical basin-to-basin connections through a series of simulation experiments.

#### a. Tropical–extratropical connection

We begin by examining the influence that midlatitudes may have on the Tropics and vice versa through identification of the forcing that establishes the distribution of anomalies in each region in the Atlantic. Here we explore the influence of the North Atlantic on the tropical Atlantic by similarly regressing the forcing fields on the North Atlantic Oscillation (NAO) index, a proxy for fluctuations in the midlatitude storm tracks, to construct seasonally varying anomalous forcing fields, which can be obtained from the National Oceanic and Atmospheric Administration (NOAA) Climate Prediction Center (<http://www.cpc.ncep.noaa.gov/data/teledoc/teletab.gif>). We expect the NAO to exert its greatest influence during the seasons of October–December (OND) when it is strongest and March–May (MAM) when the variability of the ITCZ is greatest. Interestingly, maximum regressed SST anomalies on the NAO index barely reach the magnitude of  $0.1^{\circ}\text{C}$  in the subtropics with no appreciable effect on surface pressure gradients south of  $25^{\circ}\text{N}$  during either season.

In general we find, consistent with Sutton et al. (2000a), that the simulated NAO wind anomalies do not have large amplitudes south of  $\sim 15^{\circ}\text{N}$  during winter and spring. Our results do indicate that a positive NAO

index is associated with positive basinwide sea level pressure anomalies and zonal surface wind anomalies in the northern subtropics. Additional simulations when the model is forced with only anomalous diabatic heating or when it is forced with only anomalous transients reveal that those forcing terms are equally important in producing anomalies of sea level pressure and 200-mb geopotential height in the subtropics. Transients are needed to extend the response west of  $60^{\circ}\text{W}$ .

Next we examine the impact of tropical anomalies on midlatitude circulation during boreal spring and summer, the seasons of maximum amplitude of the tropical Atlantic anomalies. When forcing is limited to the tropical Atlantic (Figs. 4b,d) there is only a weak response in the northern extratropics. For the interhemispheric distribution of anomalies there is a southwest–northeast wavelike pattern from the northern tropical Atlantic extending through northern Africa and Eastern Europe to northern Asia during spring. For the equatorial distribution of anomalies the propagation is in a northwest–southeast direction from the southern tropical Atlantic through the Antarctic Ocean (south of Africa) extending to Antarctica during boreal summer (i.e., austral winter). This result differs from the stronger (boreal) wintertime response discussed by Robertson et al. (2000) and Watanabe and Kimoto (1999). In both cases the extratropical response is barotropic in structure, as observed (Ruiz-Barradas et al. 2002).

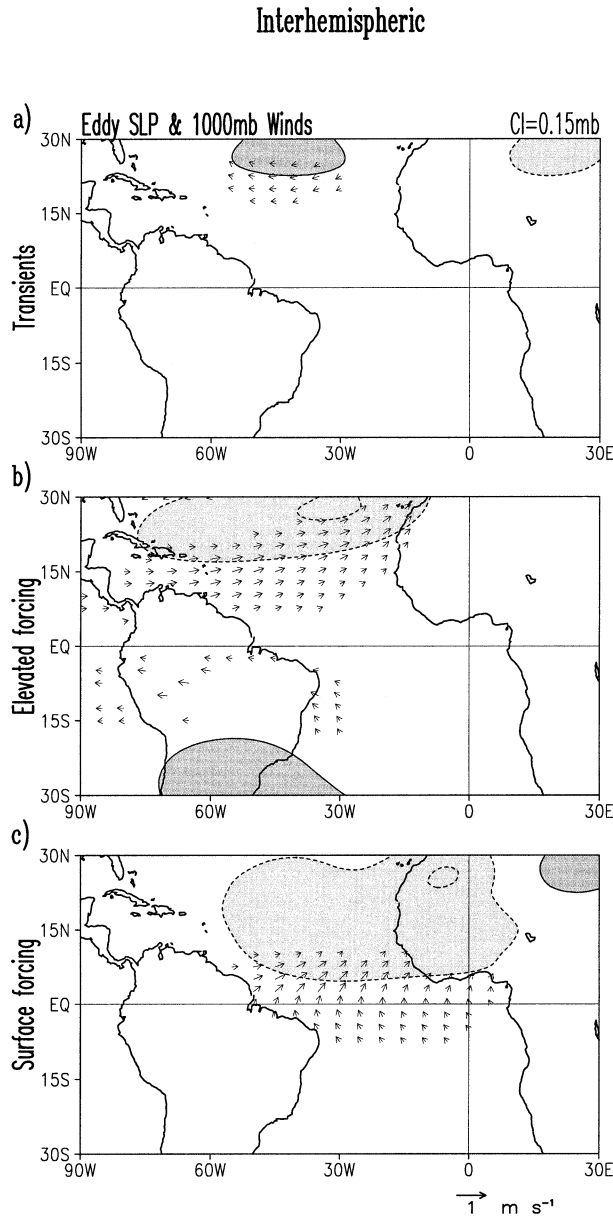


FIG. 7. Simulations examining the impact of anomalous diabatic heating and transients in the tropical Atlantic for the interhemispheric distribution of anomalies. Eddy anomalies of sea level pressure (mb) and wind ( $\text{m s}^{-1}$ ) at 1000 mb when (a) only anomalous momentum and thermal transients, (b) only anomalous mid- and upper-level diabatic heating (pressure  $\leq 690$  mb), and (c) only anomalous diabatic heating at lower levels (pressure  $\geq 780$  mb) and surface temperature force the model. Dark (light) shading denotes positive (negative) anomalies larger than  $\pm 0.15$  mb for pressure and  $\pm 2 \times 10^{-7} \text{ s}^{-1}$  for divergence.

#### b. Pacific–Atlantic interaction

As indicated in the introduction ENSO induces circulation patterns during boreal spring that resemble those associated with the interhemispheric distribution of anomalies. Two main mechanisms have been proposed to explain this ENSO influence, a direct modi-

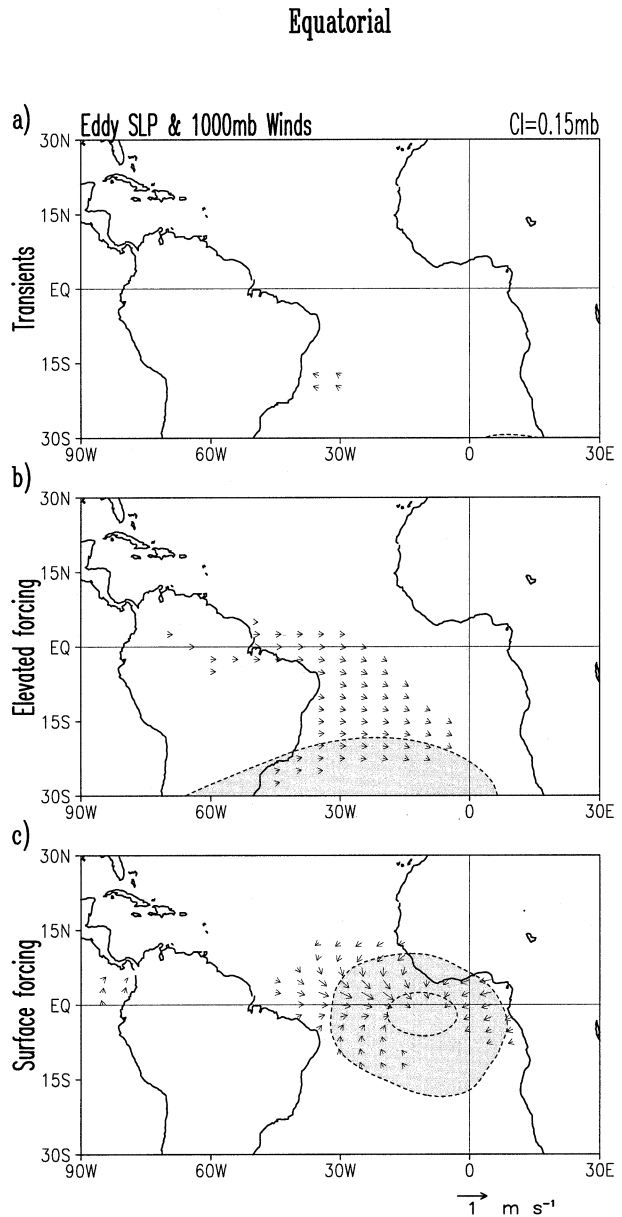


FIG. 8. The same as in Fig. 7 but for the equatorial distribution of anomalies.

fication of the Atlantic Walker circulation and an indirect modification of the northern tropical Atlantic winds through changes in the midlatitudes. Here we examine both mechanisms.

To distinguish between the response of the Atlantic atmosphere to locally generated anomalies from the response to ENSO-generated anomalies in the tropical Pacific, we first obtain forcing by regression against the Kaplan extended Niño-4 ( $5^{\circ}\text{N}$ – $5^{\circ}\text{S}$ ,  $150^{\circ}\text{W}$ – $160^{\circ}\text{E}$ ) SST index (Kaplan et al. 1998) during boreal spring (MAM), the season of maximum connection between the basins (Enfield and Mayer 1997). Then we compare the regressed surface and 200-mb fields with those simulated

## Interhemispheric

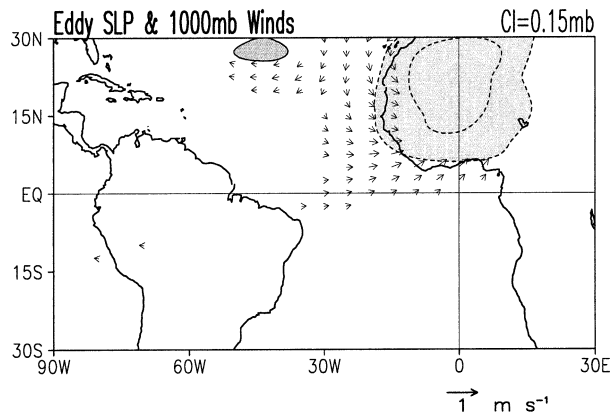


FIG. 9. Simulation examining the impact of anomalous diabatic heating over the continents in the tropical Atlantic for the interhemispheric distribution of anomalies. Eddy anomalies of sea level pressure (mb) and wind ( $\text{m s}^{-1}$ ) at 1000 mb when anomalous diabatic heating and surface temperatures are confined over the contiguous continents but transients exist in the whole tropical Atlantic domain. Climatological conditions are imposed in the rest of the global domain. Dark (light) shading denotes positive (negative) anomalies larger than  $\pm 0.15$  mb for pressure and  $\pm 2 \times 10^{-7} \text{ s}^{-1}$  for divergence.

by the model when forcing is global and when it is confined to the tropical Pacific, between  $20^{\circ}\text{S}$ – $20^{\circ}\text{N}$  and  $130^{\circ}\text{E}$ – $90^{\circ}\text{W}$  in one case, and to the western tropical Pacific, between  $20^{\circ}\text{S}$ – $20^{\circ}\text{N}$  and  $130^{\circ}\text{E}$ – $140^{\circ}\text{W}$  in another case (Figs. 11 and 12). Inclusion of orography does not improve simulations in the tropical Atlantic domain. Although the global simulation is quite good, there are quantitative errors; for example, the upper-level Aleutian trough partially fails to connect across the United States as suggested by the upper-level circulation and reflected on the sea level pressure anomalies (Fig. 11).

When the forcing is confined only into the tropical Pacific between  $20^{\circ}\text{S}$ – $20^{\circ}\text{N}$  and  $130^{\circ}\text{E}$ – $90^{\circ}\text{W}$  (Figs. 12a,b) the simulation reveals an equatorial response in the Atlantic through changes in the Walker circulation, and the lack of anomalies at surface and upper levels from the subtropical Atlantic toward the poles. Wind anomalies in the tropical Atlantic are largely zonal at both levels (easterly at surface and westerly at 200 mb) while upper-level convergence anomalies over northern South America and along the equatorial Atlantic are at their minimum and zonally oriented. With no negative sea level pressure anomalies in the northern subtropical Atlantic, and with no upper-level divergence anomalies in the western tropical Atlantic, surface and upper-level wind anomalies are also mainly zonal. The easterly equatorial surface wind anomalies have the potential for cooling the upper layer of the ocean by inducing anomalous upwelling.

A comparison of the previous tropical Pacific simu-

## Global Forcing

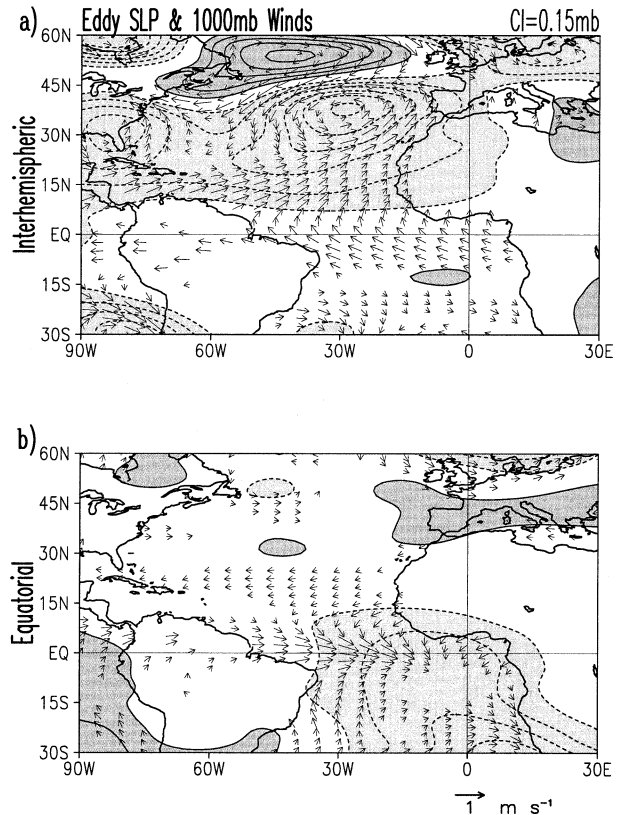


FIG. 10. Simulations examining the impact of global forcing on the tropical Atlantic. Anomalous diabatic heating, momentum and thermal transients, and surface temperature are global. Eddy anomalies of sea level pressure (mb) and wind ( $\text{m s}^{-1}$ ) at 1000 mb for the (a) interhemispheric distribution of anomalies and (b) equatorial distribution of anomalies. Dark (light) shading denotes positive (negative) anomalies larger than  $\pm 0.15$  mb.

lation with the one in which global forcing is used (Figs. 11c,d), may suggest that the upper-level midlatitude trough and associated winds are responsible for intensification of the upper-level divergence anomalies over the Caribbean Sea and contribute to the divergence anomalies in the northern Tropics. This midlatitude interaction has also been suggested by Sutton et al. (2000a) during winter rather than spring. However if forcing is confined to the north of  $20^{\circ}\text{N}$  over the Pacific only (not shown), the response is mostly confined to the west of  $70^{\circ}\text{W}$  over the Gulf of Mexico with no significant impact over the tropical Atlantic region. This result suggests that the midlatitude influence from ENSO events, from the zonally symmetric model's perspective, is weak. Interestingly when forcing is constrained to the Pacific west of  $140^{\circ}\text{W}$  (Figs. 12c,d) the response in the Atlantic is confined to the latitude band  $10^{\circ}$ – $15^{\circ}\text{N}$  with southwesterly surface wind anomalies. From this last simulation it is clear that heating anomalies in the east-



### Pacific–Atlantic link (MAM)

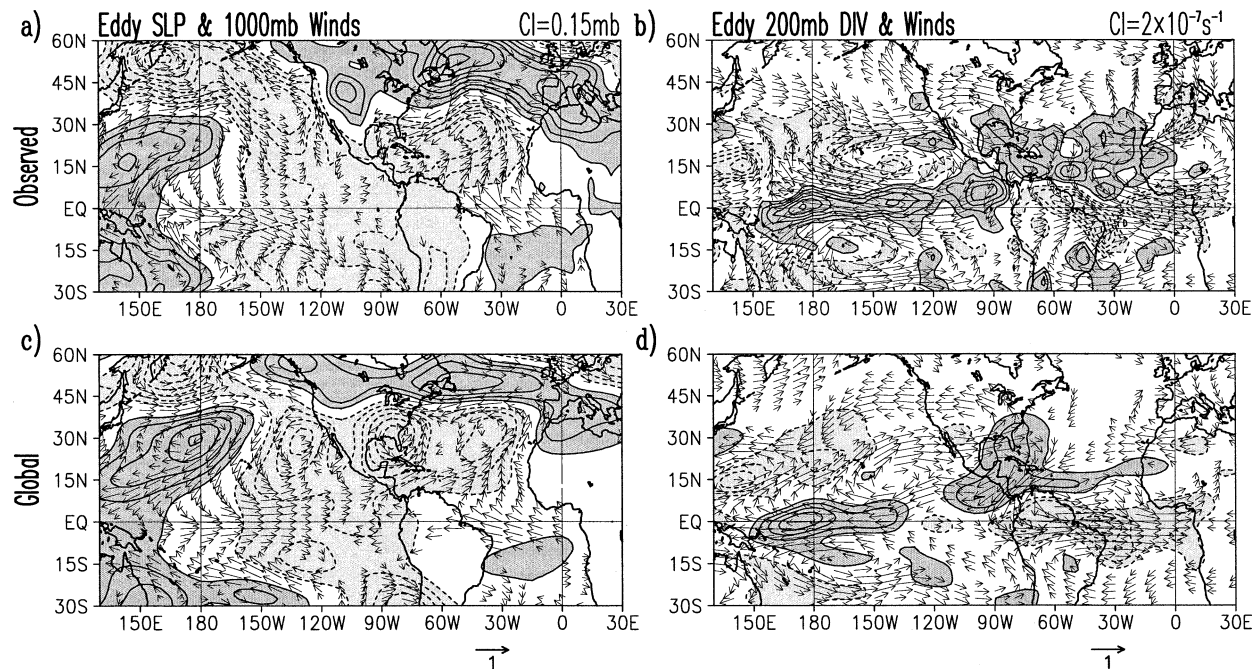


FIG. 11. Simulations exploring the tropical Pacific–tropical Atlantic link during Mar–May (MAM). Forcing (anomalous diabatic heating, momentum and thermal transients, and surface temperatures) is derived from the regressed Niño-4 index during boreal spring. (a), (c) Eddy anomalies of sea level pressure (mb) and wind ( $\text{m s}^{-1}$ ) at 1000 mb, and (b), (d) eddy anomalies of divergence ( $\text{s}^{-1}$ ) and wind ( $\text{m s}^{-1}$ ) at 200 mb. (a), (b) Regressed NCEP–NCAR reanalysis fields from MAM Niño-4 index. (c), (d) Simulation when forcing is global. Dark (light) shading denotes positive (negative) anomalies larger than  $\pm 0.15$  mb for pressure and  $\pm 2 \times 10^{-7} \text{ s}^{-1}$  for divergence.

ern Pacific contribute the most to the upper-level divergence anomalies and equatorial convergence anomalies suggesting a weaker Atlantic Hadley cell for the spring. These results are consistent with those of Chiang and Kushnir (2000), Saravanan and Chang (2000), and Mestas-Núñez and Enfield (2001), who emphasize the role of tropical interactions between the basins.

Additional simulations when the model is only forced with transients, or diabatic heating, or surface forcing, make clear that the baroclinic anomalous circulation in the Tropics is primarily the result of diabatic heating. Transients give an equivalent barotropic response in midlatitudes with the negative sea level pressure anomalies below an extended trough (crossing from the Pacific Ocean through the United States and reaching the mid-Atlantic) but with no wind anomalies south of  $15^\circ\text{N}$ . Surface forcing does not have a direct influence on tropical Atlantic circulation.

### 5. Summary and conclusions

Here, we use a diagnostic primitive equation model of the atmosphere to examine the atmospheric response to typical anomalous conditions in the tropical Atlantic sector identified at interannual and longer timescales. Anomalous diabatic heating, boundary layer tempera-

ture, and transients are specified independently based on analysis of 36 yr of atmospheric reanalysis data. In order to separate out the atmospheric role in different phenomena we decompose the forcing by calculating its projection on several index time series. For the local response we use index time series associated with interhemispheric and equatorial distribution of anomalies. For the response to remote forcing we use index time series associated with ENSO and the North Atlantic oscillation. In each case we exploit the simplicity of the model to examine the independent contribution of diabatic heating at different levels, transient and stationary fluxes, and boundary layer processes (diabatic heating at lower levels and surface temperature).

As a result of examining the local response we find that realistic diabatic heating anomalies associated with anomalous movements of the ITCZ is the most important term forcing the annual and interannual tropical Atlantic circulation and in particular, near-surface tropical Atlantic wind anomalies. We focus on this phenomenon by examining the forcing associated with a boreal spring index associated with the interhemispheric pattern of anomalies (see R-BCN). Continental heating over northwest Africa associated with this index is important in influencing wind anomalies at the surface in the northern Tropics. In contrast, continental heating

## Tropical Pacific–Atlantic link (MAM)

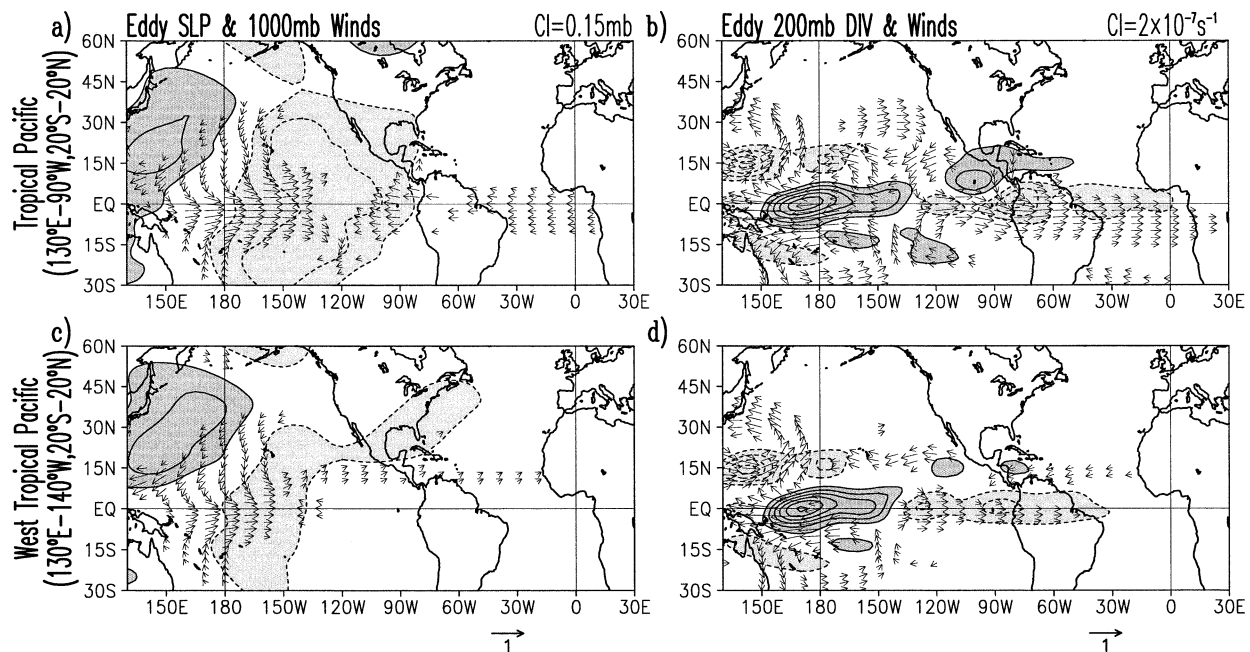


FIG. 12. Simulations exploring the tropical Pacific–tropical Atlantic link during MAM. Forcing comes from MAM Niño-4 index, and distribution of fields is the same as in Fig. 11. (a), (b) Simulation when forcing is confined to the tropical Pacific sector (20°S–20°N, 130°E–90°W) with climatological conditions in the rest of the global domain. (c), (d) Simulation similar to (a), (b) but forcing is confined to the western tropical Pacific (20°S–20°N, 130°E–140°W). Shading and contours are the same as in Fig. 11.

from the Amazon region seems less important because of the lack of surface forcing. In the deep Tropics we find, consistent with the results of Lindzen and Nigam (1987), Wu et al. (2000), Chiang et al. (2001), and others, that surface forcing is a dominant term while transients are relatively unimportant. In contrast to Chiang et al. (2001), we find that surface forcing affects both zonal and meridional components of the anomalous surface winds. Interestingly, diabatic heating anomalies within the tropical Atlantic results in a wavelike pattern extending into the northeast extratropics.

Changes in surface wind speed in response to anomalous forcing may feed back changes in latent heat flux that may alter SST in such a way as to reinforce the original anomaly (Carton et al. 1996). We find the primary zone in which this positive feedback takes place is on the western side of the basin, somewhat north of the equator, a result that is consistent with Chang et al. (2000, 2001). In the northeast the feedback has a negative sense mostly because of the correlation between wind speed and direction and the presence of moist marine or dry continental air. This latter result may be inconsistent with observations, however (WC02).

We contrast the basin response to forcing associated with the interhemispheric index in boreal spring with that associated with the equatorial index in boreal summer. The response to forcing associated with the equatorial index varies with longitude with surface forcing

dominating east of 30°W but diabatic heating anomalies above 780 mb dominating to the west as well as in the southern subtropics. For this equatorial distribution of anomalies, which was not considered in Chiang et al. (2001), the impact of surface forcing on both meridional and zonal surface wind anomalies is equally important. Equatorial forcing also induces an extratropical response, in this case extending to the southeast into the winter Southern Hemisphere.

We next consider the interactions between the tropical Atlantic and the North Atlantic by examining the response to forcing associated with the North Atlantic oscillation index in the same seasons discussed earlier, boreal spring and summer. Consistent with previous studies (Sutton et al. 2000a,b) we find the influence in the atmosphere is limited to the northern subtropics with transients playing a central role.

Next, we consider the fascinating question of the influence of ENSO on the tropical Atlantic. As discussed in the introduction, previous studies have suggested several scenarios by which such an influence may take place. Our results indicate that heating in the eastern tropical Pacific is able to 1) alter the Atlantic Walker circulation enhancing upper-level westerlies along the equator and strengthening the near-surface easterly trades, and 2) play a role maintaining the upper-level divergence between 10°–15°N and the equatorial convergence that suggests a weak Atlantic Hadley cell. This

scenario in the tropical Atlantic set up conditions for local air–sea interactions to take place. Finally we note that many of these conclusions need to be explored as well in the context of coupled models (e.g., Chang et al. 2001) because of the strong interaction among ocean, land, and atmosphere in this sector.

**Acknowledgments.** A. Ruiz-Barradas gratefully acknowledges support from the National University of Mexico. He and J. A. Carton have also been supported by the National Science Foundation (OCE9812404). S. Nigam and A. Ruiz-Barradas would like to acknowledge support of NOAA Grants NA96GP0213 and NA06GP0362. The authors also want to thank to John Chiang, David Enfield, and an anonymous reviewer for their comments, which improved the final version of the paper.

#### REFERENCES

- Bolton, D., 1980: The computation of equivalent potential temperature. *Mon. Wea. Rev.*, **108**, 1046–1053.
- Carton J. A., X. Cao, B. S. Giese, and A. M. da Silva, 1996: Decadal and interannual SST variability in the tropical Atlantic Ocean. *J. Phys. Oceanogr.*, **26**, 1165–1175.
- Chang, P., R. Saravanan, L. Ji, and G. C. Hegerl, 2000: The effect of local sea surface temperatures on atmospheric circulation over the tropical Atlantic sector. *J. Climate*, **13**, 2195–2216.
- , L. Ji, and R. Saravanan, 2001: A hybrid coupled model study of tropical Atlantic variability. *J. Climate*, **14**, 361–390.
- Chiang, J. C. H., and Y. Kushnir, 2000: Interdecadal changes in eastern Pacific ITCZ variability and its influence on the Atlantic ITCZ. *Geophys. Res. Lett.*, **27**, 3687–3690.
- , S. E. Zebiak, and M. A. Cane, 2001: On the relative role of elevated heating and surface temperature gradients in driving anomalous surface winds over tropical oceans. *J. Atmos. Sci.*, **58**, 1371–1394.
- Chung, C., S. Nigam, and J. A. Carton, 2002: SST-forced surface wind variability in the tropical Atlantic: An empirical model. *J. Geophys. Res.*, **107**, 4244, doi:10.1029/2001JD000324.
- Curtis, S., and S. Hastenrath, 1995: Forcing of anomalous sea surface temperature evolution in the tropical Atlantic during Pacific warm events. *J. Geophys. Res.*, **100**, 15 835–15 847.
- Enfield, D. B., and D. A. Mayer, 1997: Tropical Atlantic SST variability and its relation to El Niño–Southern Oscillation. *J. Geophys. Res.*, **102**, 929–945.
- Giannini, A., Y. Kushnir, and M. A. Cane, 2000: Interannual variability of Caribbean rainfall, ENSO, and the Atlantic Ocean. *J. Climate*, **13**, 297–311.
- Hastenrath, S., 1978: On modes of tropical circulation and climate anomalies. *J. Atmos. Sci.*, **35**, 2222–2231.
- , and L. Greischar, 1993: Circulation mechanisms related to northeast Brazil rainfall anomalies. *J. Geophys. Res.*, **98**, 5093–5102.
- Held, I. M., S. W. Lyons, and S. Nigam, 1989: Transients and the extratropical response to El Niño. *J. Atmos. Sci.*, **46**, 163–174.
- Kalnay, E., and Coauthors, 1996: The NMC/NCAR 40-Year Reanalysis Project. *Bull. Amer. Meteor. Soc.*, **77**, 437–471.
- Kaplan, A., M. Cane, Y. Kushnir, A. Clement, M. Blumenthal, and B. Rajagopalan, 1998: Analyses of global sea surface temperature 1856–1991. *J. Geophys. Res.*, **103**, 18 567–18 589.
- Lindzen, R. S., and S. Nigam, 1987: On the role of sea-surface temperature gradients in forcing low-level winds and convergence in the Tropics. *J. Atmos. Sci.*, **44**, 2418–2436.
- Mestas-Núñez, A. M., and D. B. Enfield, 2001: Eastern equatorial Pacific SST variability: ENSO and non-ENSO components and their climatic associations. *J. Climate*, **14**, 391–402.
- Moura, A. D., and J. Shukla, 1981: On the dynamics of the droughts in northeast Brazil: Observations, theory and numerical experiments with a general circulation model. *J. Atmos. Sci.*, **38**, 2653–2675.
- Nigam, S., 1994: On the dynamical basis for the Asian summer monsoon rainfall–El Niño relationship. *J. Climate*, **7**, 1750–1771.
- , 1997: The annual warm to cold phase transition in the eastern equatorial Pacific: Diagnosis of the role of stratus cloud-top cooling. *J. Climate*, **10**, 2447–2467.
- Nobre, P., and J. Shukla, 1996: Variations of sea surface temperature, wind stress, and rainfall over the tropical Atlantic and South America. *J. Climate*, **9**, 2464–2479.
- Peixoto, J. P., and A. H. Oort, 1995: *Physics of Climate*. 4th ed. American Institute of Physics, 520 pp.
- Philander, 1990: *El Niño, La Niña and the Southern Oscillation*. International Geophysics Series, Vol. 46, Academic Press, 293 pp.
- Rajagopalan, B., Y. Kushnir, and Y. M. Tourre, 1998: Observed mid-latitude and tropical Atlantic climate variability. *Geophys. Res. Lett.*, **21**, 3967–3970.
- Robertson, A. W., C. R. Mechoso, and Y.-J. Kim, 2000: The influence of Atlantic sea surface temperature anomalies on the North Atlantic oscillation. *J. Climate*, **13**, 122–138.
- Rodó, X., 2001: Reversal of three global atmospheric fields linking changes in SST anomalies in the Pacific, Atlantic and Indian oceans at tropical latitudes and midlatitudes. *Climate Dyn.*, **18**, 203–217.
- Ruiz-Barradas, A., J. A. Carton, and S. Nigam, 2000: Structure of interannual-to-decadal climate variability in the tropical Atlantic sector. *J. Climate*, **13**, 3285–3297.
- , —, and —, 2002: Response of the atmosphere to climate variability in the tropical Atlantic. *Eos, Trans. Amer. Geophys. Union*, **83** (Spring Meeting Suppl.), Abstract GC51B-09. [Poster presentation available from A. Ruiz-Barradas, 3420 Computer and Space Sciences Building, Department of Meteorology, University of Maryland, College Park, MD 20742-2425.]
- Saravanan, R., and P. Chang, 2000: Interaction between tropical Atlantic variability and El Niño–Southern Oscillation. *J. Climate*, **13**, 2177–2194.
- Sutton, R. T., S. P. Jewson, and D. P. Rowell, 2000a: The elements of climate variability in the tropical Atlantic region. *J. Climate*, **13**, 3261–3284.
- , W. A. Norton, and S. P. Jewson, 2000b: The North Atlantic Oscillation—What role for the ocean? *Atmos. Sci. Lett.*, **1**, 89–100.
- Tanimoto, Y., and S.-P. Xie, 1999: Ocean–atmospheric variability over the Pan-Atlantic basin. *J. Meteor. Soc. Japan*, **77**, 31–46.
- Wagner, R. G., and A. M. da Silva, 1994: Surface conditions associated with anomalous rainfall in the Guinea coastal region. *Int. J. Climatol.*, **14** (2), 179–199.
- Wang, C., and D. Enfield, 2001: The tropical Western Hemisphere warm pool. *Geophys. Res. Lett.*, **28**, 1635–1638.
- Wang, J., and J. Carton, 2002: Modeling climate variability in the tropical Atlantic atmosphere. *J. Climate*, in press.
- Watanabe, M., and M. Kimoto, 1999: Tropical–extratropical connection in the Atlantic atmosphere–ocean variability. *Geophys. Res. Lett.*, **26**, 2247–2250.
- Wu, Z. H., E. S. Sarachik, and D. S. Battisti, 2000: Vertical structure of convective heating and the three-dimensional structure of the forced circulation on an equatorial beta plane. *J. Atmos. Sci.*, **57**, 2169–2187.
- Zebiak, S. E., 1993: Air–sea interaction in the equatorial Atlantic region. *J. Climate*, **6**, 1567–1586.